PROCEEDINGS of the
23rd International Congress on Acoustics
9 to 13 September 2019 in Aachen, Germany

Electrostatic all silicon MEMS speakers for in-ear audio applications – acoustic measurements and modelling approach

Lutz EHRIG[(1)], Franziska WALL[(1)], Herman SCHENK[(1)], Sergiu LANGA[(1,2)], Anton MELNIKOV[(1)], Michael STOLZ[(1)], Bert KAISER[(1)], Holger CONRAD[(1)], Harald SCHENK[(1,2)]

[(1)]Fraunhofer Institute for Photonic Microsystems IPMS, Dresden, Germany, Lutz.Ehrig@ipms.fraunhofer.de
[(2)]Brandenburg University of Technology Cottbus - Senftenberg, Cottbus, Germany

Abstract
This paper presents the acoustic properties of an electroacoustic MEMS transducer. The transducer is based on electrostatic bending actuators with lateral deflection. A large number of actuators is arranged in pairs and move in opposite phase between a cover and a handle wafer. By means of an appropriate sound guidance, areas of opposite phase pressure changes are separated and audible sound is emitted. In this paper, the results of acoustic measurements with a standard ear simulator are discussed. A linear lumped parameter model is presented and the results of the simulations are compared with the measurements.
Keywords: MEMS, Speaker, Electrostatic, Headphone, Hearable

1 INTRODUCTION

Common macroscopic electrostatic transducers need high voltages due to the comparatively large gap between the electrodes. The voltage can be reduced by reducing the gap, but this in turn limits the maximum excursion of the diaphragm and consequently the maximum achievable sound pressure level.

Using micro-electro-mechanical systems (MEMS) this limitation can be overcomed by designing electrostatic actuators with very small electrode gaps. By using a force-transforming mechanism, sufficient mechanical deflection and volume displacement can be provided.

The scale of MEMS and the techniques used for fabrication lead to further distinct features: predominantly the batch fabrication and the usability of common CMOS processes resulting in low costs per unit in mass production. The small size and light weight of the devices are obvious advantages as are the high energy efficiency – at least regarding electrostatic and piezoelectric devices –, the enhanced performance and reliability and the tight tolerances that can be obtained.

A challenge in the development of MEMS devices and the testing of different designs is the long production time. It is therefore necessary to use models and simulations to identify critical properties and to optimize the MEMS design in advance.

2 "NANOSCOPIC ELECTROSTATIC DRIVE"-TECHNOLOGY (NED) FOR IN EAR AUDIO APPLICATIONS

In order to solve the contradiction between small electrode gap/low voltage and a large deflection, an electrostatic bimorph bending actuator has been developed at Fraunhofer IPMS. A particular design of the electrodes enables a transformation of the electrostatic force, which, in conjunction with a lever mechanism, allows deflections to be generated that are significantly larger than the gap itself.

The actuator consists of two non-planar electrodes separated by insulating spacers as depicted in Fig. 1a. In case of an electrical potential V between the top (green) and the bottom (gray) electrodes an electrostatic field E is generated, which leads to the attraction of the electrodes due to the Coulomb force. Because of the roof-like topography of the top electrode, the attraction results in a lateral strain and a force F leading to a downward

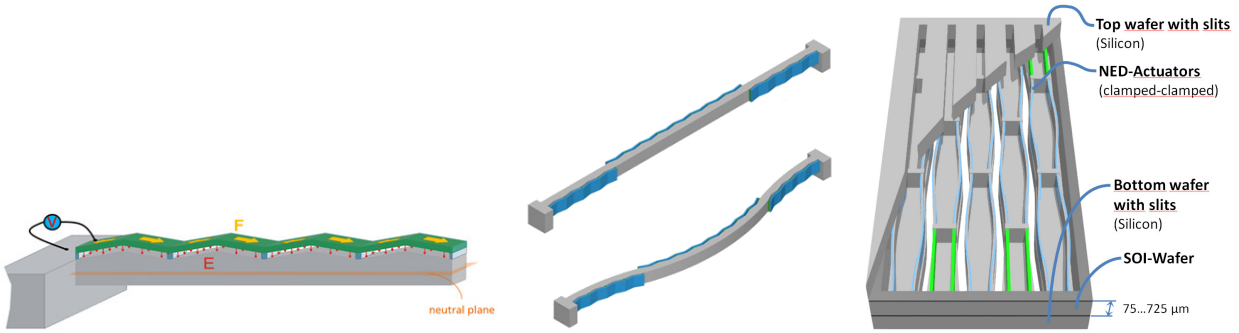

(a) (b) (c)

Figure 1. (a) Electrostatic bending actuator "Nano Electrostatic Drive" (NED): An electric potential V between two electrodes results in a force F, which – due to the topology of the electrodes – results in a bending of the beam. (b) Clamped-clamped NED-actuators in rest position (upper beam) and with a S-shaped deflection curve (lower beam). (c) NED audio transducer chip with multiple clamped-clamped actuators and a top and a handle wafer with vents. The beams are shown in the deflected state.

bending of the cantilever tip. Shifting the spacers to the top of the roof-like-structured electrodes, an upward bending can be achieved. The actuator mechanism is described in detail in [1].

The NED actuators are clamped on both sides and structured in a way that an S-shaped deformation occurs, see Fig. 1b. Beams with opposite deflection curves are arranged in pairs, so that the volume between them changes according to the applied signal voltage. Multiple pairs of actuators are arranged on a chip, see Fig. 1c. The device layer is between a top and a handle wafer each of them having vents to release the air. Separating the front and the back side of the chip, the acoustic short circuit is avoided and the chip emits audible sound.

3 ACOUSTICAL MEASUREMENTS

3.1 Test Structure

A test structure – optimized for the audible frequency range – is depicted in Fig. 2a. It contains three sub-chips with a size of approx. $6.2 \times 2.4\,\mathrm{mm}^2$ each and an active area of $5.5 \times 1.7\,\mathrm{mm}^2$ respectively. The bond wires to the printed circuit board are visible and on top of each sub-chip, the cover with the air vents can be seen.

A microscopic image of the beams of one sub-chip is shown in Fig. 3. The sub-chip consists of 14 pairs of beams with a length of 2200 µm and seven pairs of short beams with a length of 1100 µm as a fill-in. The mechanical behavior of both types of beams is different, but due to the ratio of 4:1 regarding the total length of long beams and total length of short beams, it is safe to assume that the long beams dominate the acoustic characteristics.

The sub-chip is subdivided into three actuator groups. Group 1 and 3 have the same number of actuators: six pairs of long beams and three pairs of short beams. Group 2 has two pairs of long beams and one pair of short beams.

In Fig. 2b an illustration of the cross section of the chip with one pair of beams is shown. The height of the beams is 75 µm, the height of the top wafer and the handle wafer is 400 µm. The clearance, i.e. the gap between the beams and the handle wafer and the top wafer, is 1 µm respectively.

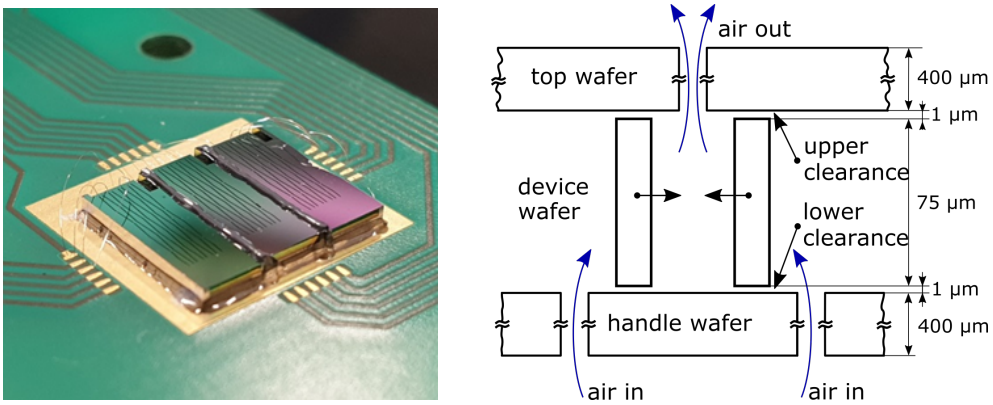

(a) (b)

Figure 2. (a) Test structure of a NED audio transducer with three sub-chips, each having an active area of $5.5 \times 1.7\,\mathrm{mm}^2$. (b) Cross section of the chip showing one pair of beams and the vents for the air in the top and in the handle wafer. The arrow direction for the movement of the beams and the air flow shows the first half of a vibration period.

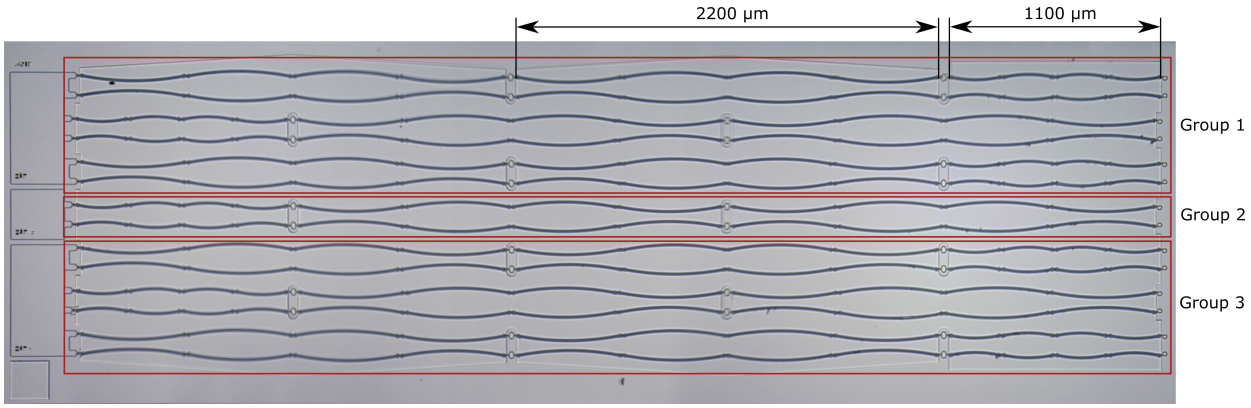

Figure 3. Stitched microscopic image of one sub-chip of the test structure (without a top cover and with a handle wafer without vents). The sub-chip is composed of 14 pairs of beams with a length of 2200 µm and seven pairs of beams with a length of 1100 µm. The sub-chip is split in 3 groups.

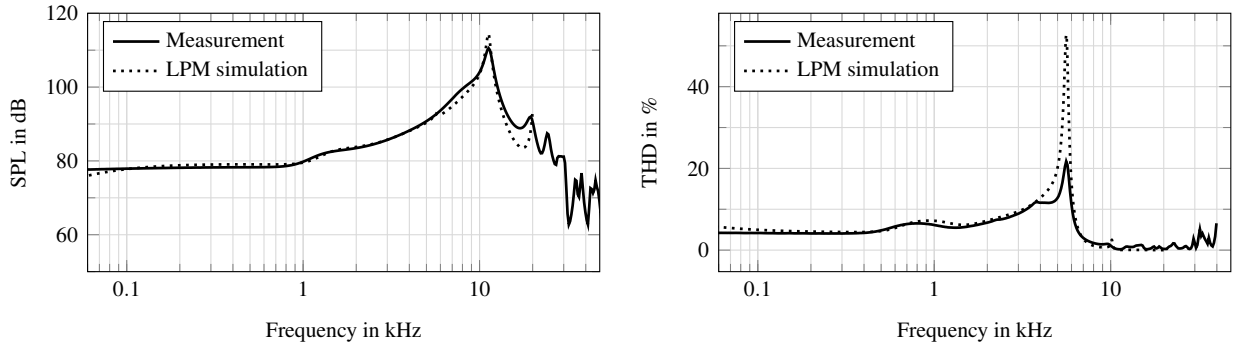

Figure 4. Sound pressure level (a) and total harmonic distortion (b) measured (solid line) and simulated (dotted line) of a test structure with three sub-chips.

3.2 Measurement Setup

The rear side of the test structure was measured through a hole in the printed circuit board (PCB) with an ear simulator (GRAS RA0045, in accordance to IEC 60318-4, with a Microtech Gefell MV210 preamplifer) directly attached to the PCB. The front side of the chip remained free. Measurement signals were generated and analyzed by an audio analyzer system (NTI Audio Flexus FX100). The amplification of the generator signal and the bias voltage were provided with an amplifier (Krohn-Hite 7602M).

3.3 Measurement Results

The results of the sound pressure level and total harmonic distortion measurements are shown in Fig. 4. All three sub-chips were measured simultanously with a bias voltage of 40 V and a signal voltage of 10 Vpp.

The frequency response of the sound pressure level in Fig. 4a is dominated by the transfer function of the ear simulator showing a steady rise of the curve above 1 kHz and the $\frac{\lambda}{2}$-resonance of the main coupler volume at 11.3 kHz. The SPL at the almost flat low frequency region is between 77 dB and 80 dB at 20 Hz and 1 kHz respectively. The slight bump around 8 kHz is due to the mechanical resonance of the NED transducer.

The total harmonic distortion, shown in Fig. 4b, is dominated by the 2nd harmonic due to the quadratic relation between signal voltage and displacement.

4 MODELING

In Fig. 5 the equivalent electrical circuit of our model is shown, with the electrical domain on the left, the mechanical domain in the center and the acoustical domain on the right. All domains are connected through a transduction element representing the eneregy transfer between them. The device behavior is thereby described at a working point, defined by the DC-voltage, for small periodic oscillations caused by the AC-voltage. In order to keep the logic of two-port theory forces are linearized around this working point. Further, a time-independent energy-transfer is assumed. The electric domain represents the outer electric circuit. Here, the series resistor takes the voltage source's internal resistance into account. Leakage currents are summed up in the parallel resistor.

The transduction element describes the energy transfer from the electric towards the mechanical domain and is therefore derived from the following equation of motion,

$$m\frac{\mathrm{d}^2x(t)}{\mathrm{d}t^2}+r\frac{\mathrm{d}x(t)}{\mathrm{d}t}+k_0(x_0+x(t))=\frac{1}{2}\varepsilon_0\varepsilon_\mathrm{r}A\frac{U^2}{(g_0-(x_0+x(t)))^2}. \tag{1}$$

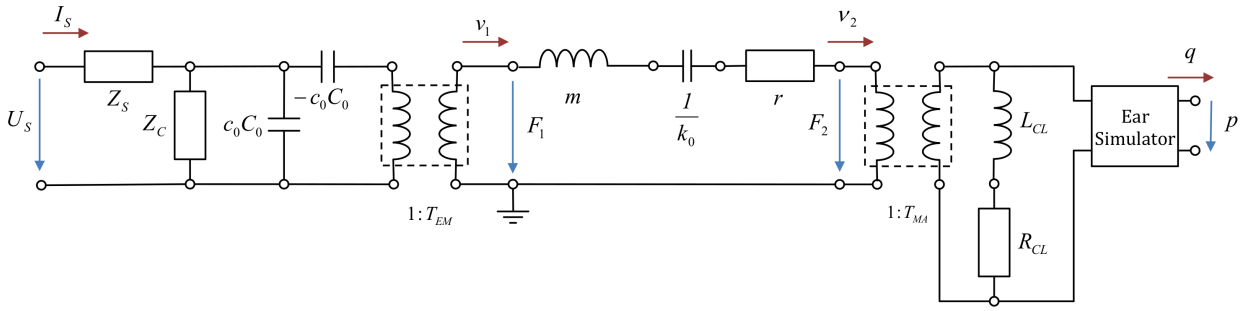

Figure 5. Equivalent electrical circuit of the model for our electrostatic transducer.

Here, we assume a damped mass-spring-system combined with a parallel plate capacitor with one movable electrode. This movement of a mass m is described in the displacement $x(t)$ around the equilibrium position x_0 caused by the applied DC-voltage. The elastic force is described with a spring constant k_0. On the other side, the Coulomb force of a plate capacitor is defined by the vacuum permeability ε_0, the relative permeability ε_r, the electrodes area A, the gapsize g_0 and the voltage U with an DC-part U_{DC} and a AC-part $U_{AC}\cos(\omega t)$ with the electric oscillation frequency ω. For the equivalent network each force is linearized around the working point x_0,

$$F_{\text{Spring}} = k_0 x_0 + k_0 x(t), \tag{2}$$

$$F_{\text{Coulomb}} \approx \frac{1}{2}\varepsilon_0 \varepsilon_r A U^2 \left(\frac{1}{(g_0 - x_0)^2} + \frac{2x(t)}{(g_0 - x_0)^3} \right). \tag{3}$$

The static equilibrium leads to a cancellation of the constant offset by the Coulomb as well as spring force. The remaining amplitude of the electrostatic force due to the AC-voltage defines the energy transduction coefficient T_{EM} which depends on the initial transducer capacity C_0 scaled with the additional DC-offset of the displacement,

$$T_{\text{EM}} = U_{\text{DC}} \frac{c_0^2 C_0}{g_0} \text{ with } c_0 = \frac{g_0}{g_0 - x_0}. \tag{4}$$

Further, the second harmonic is generated by the squared AC-voltage with its own transduction coefficient. The conversion of current into velocity v results in an additional parallel capacitor on the electric side through the time derivative of the voltage.

$$I \approx U_{\text{DC}} \frac{\mathrm{d}C(t)}{\mathrm{d}t} + c_0 C_0 \frac{\mathrm{d}U(t)}{\mathrm{d}t} = U_{\text{DC}} \frac{\mathrm{d}C}{\mathrm{d}x} v + i\omega c_0 C_0 U_{\text{AC}}. \tag{5}$$

In the mechanical domain forces are equivalent to voltages and thereby a mass to a inductance, damping to a resistance and a spring to a capacitor. In our system the electrostatic force is opponent to the elastic force leading to a softening for the effective spring constant k_{eff} of the complete system. The linear part of the Coulomb force determines k_{eff} and makes it thereby depending on the working point,

$$k_{\text{eff}} = k_0 - \Delta k_{\text{Coulomb}} = k_0 - \frac{1}{2}\varepsilon_0 \varepsilon_r A U_{\text{DC}}^2 \frac{2}{(g_0 - x_0)^3} = k_0 - \frac{T_{\text{EM}}^2}{c_0 C_0}. \tag{6}$$

This effect is accomplished in the negative series capacitance within the electric domain in order to get a purely mechanical domain. The complete transducer system is modeled by parallel connected damped spring-mass systems.

The force within the mechanical domain is transfered into a pressure scaled with the swept area. Here, we approximate this area by the beam with a triangular shape. The two ports on the right of the mechano-acoustical

coupling transformer represent the front and the back side of the NED beams in the chip. The clearance of 1 µm, which is a fluidic connection between the front and the back side of the beams (see Fig. 3), is modeled by a parallel branch of the coupling transformer consisting of an inductance L_{CL} in series with a resistor R_{CL} with the impedance given in [2]. It has to be taken into account that the clearance occurs twice, once above and once below the beams. In order to compare this model to presented experiments the system's equivalent circuit is extended at the acoustic domain with an ear simulator according to IEC 60318-4 [3]. The measured SPL corresponds to the pressure generated by the fundamental mode p_1. The conversion between voltage and pressure is calculated with the equivalent network. This pressure is used to determine the corresponding sound pressure level,

$$SPL = 20\log_{10}(\frac{p_1}{p_{\mathrm{ref}}}). \tag{7}$$

For THD the second harmonic's pressure p_2 is compared to the sum of the fundamental and the second mode,

$$THD = 100\sqrt{\frac{p_2^2}{p_1^2+p_2^2}}. \tag{8}$$

5 CONCLUSION AND FUTURE WORK

The presented micro speaker is based on a multitude of bimorph-like electrostatic bending actuators. The actuators are arranged between a vented handle and cover wafer and are designed to emit sound in the audible frequency range.

Measurement results of a test structure were presented proving audio reproduction capabilities for in-ear audio applications. Below resonance sound pressure levels between 77 dB and 80 dB were measured in an IEC 60318-4 ear simulator with a THD of 5 %. Harmonic distortions are dominated by second-order products.

A simple lumped parameter model based on a mass-spring-system combined with a parallel plate capacitor was presented. The simulation results of the model for SPL and THD were presented and are in good agreement with the measurements.

Further development focuses on increasing sound pressure level and linearity by optimizing the actuator design. To make efficient use of the long production times in the clean room developing and refining the models of the transducer is an ongoing task combining the results of analytical calculations, FEM simulations and knowledge gained from electrical, optical and acoustical measurements.

ACKNOWLEDGEMENT

The work shown here was funded in the project MEMSound by the German Federal Ministry of Education and Research (BMBF) in the funding measure "Validation of the technological and social innovation potential of scientific research - VIP +" under the grant number 03VP01800.

REFERENCES

[1] Conrad, H.; et al. A small-gap electrostatic micro-actuator for large deflections. Nature Communications, 2015, doi:10.1038/ncomms10078.

[2] Beranek, L. Acoustics. Acoustical Society of America, 1993 (1954).

[3] Brüel& Kjær, Application Note Ear Simulator for Telephonometry, Denmark, 2012.